First-principles study on lithium amide for hydrogen storage

Kazutoshi Miwa,* Nobuko Ohba, and Shin-ichi Towata
Toyota Central Research & Development Laboratories, Inc., Nagakute, Aichi 480-1192, Japan

Yuko Nakamori and Shin-ichi Orimo
Institute for Materials Research, Tohoku University, Sendai 980-8577, Japan
(Received 30 November 2004; published 20 May 2005)

The fundamental properties of lithium amide $LiNH_2$, which is fully hydrogenated phase of lithium nitride Li_3N, have been investigated by the first-principles calculations using the ultrasoft pseudopotential method, including the structural, electronic, dielectric, and vibrational properties. The calculated structural parameters agree well with the experimental data except for hydrogen positions. The analyses for the electronic structure and the Born effective charge tensors indicate an ionic feature between Li^+ and $[NH_2]^-$. The internal bonding of $[NH_2]^-$ anions is primarily covalent. The internal N-H bending and stretching vibrations of $[NH_2]^-$ anions yield Γ-phonon modes around 1500 and 3400 cm^{-1}, respectively. These can be fairly reproduced by the molecular approximation, suggesting a strong internal bonding of $[NH_2]^-$ anions. The heat of formation for the fully hydriding reaction of Li_3N is predicted as -85 kJ/mol H_2 which agrees well with the experimental value. Some discussions are also presented for the properties of Li_3N.

DOI: 10.1103/PhysRevB.71.195109 PACS number(s): 71.20.Ps, 61.66.Fn, 63.20.Dj

I. INTRODUCTION

Complex hydrides have been noticed as one of the most promising materials for hydrogen storage due to their high gravimetric densities of hydrogen. Bogdanović and Schwickardi have first reported that the catalyzed sodium alanate ($NaAlH_4$) shows reversible hydriding and dehydriding reactions at moderate temperatures.[1] Motivated by this report, many attempts have been tried to enhance the reversibility of the hydriding and dehydriding reactions for alkali-metal complex hydrides.[2–10] Lately, Chen *et al.*[11] have shown that lithium nitride exhibits the following two-step reversible reactions with gaseous hydrogen without any aid of external catalysts:

$$Li_3N + 2H_2 \leftrightarrow Li_2NH + LiH + H_2 \leftrightarrow LiNH_2 + 2LiH. \quad (1)$$

The products of two-step reactions are lithium imide (Li_2NH) and lithium amide ($LiNH_2$) with by-products of lithium hydride, respectively, where 10.4 mass % of hydrogen is stored in the overall reactions. The dehydriding reaction starts mainly about 473 K in vacuum. Although the operation temperature is still too high, the large amount of reversible hydrogen is encouraging for applications.

Theoretical investigations using first-principles calculations are very helpful to understand the fundamental properties of materials. We have recently performed first-principles calculations on $LiBH_4$,[12] which is a potential candidate for hydrogen storage because of its extremely high hydrogen content of 18.5 mass %. The analyses indicate that the charge compensation by Li^+ is a key feature for the stability of the internal bonding of $[BH_4]^-$ anions and so it is expected that the suppression of the charge transfer by partial substitution of more electronegative elements for Li is effective to lower the dehydriding temperature. This idea has been examined theoretically in the case of copper as a substituent element.[13] Understanding the fundamental properties of $LiNH_2$ and Li_2NH from a theoretical point of view will be also beneficial for improving their performance. To this end, we have performed the first-principles calculations on $LiNH_2$ to predict its fundamental properties and have published the results very briefly.[14] In this paper, we report the detailed results of the first-principles calculations on $LiNH_2$ including the structural, electronic, dielectric, and vibrational properties. Some discussions are also presented for the properties of Li_3N which is a starting material for the hydriding reaction and is also of interest from the viewpoint of a superionic conductor.[15]

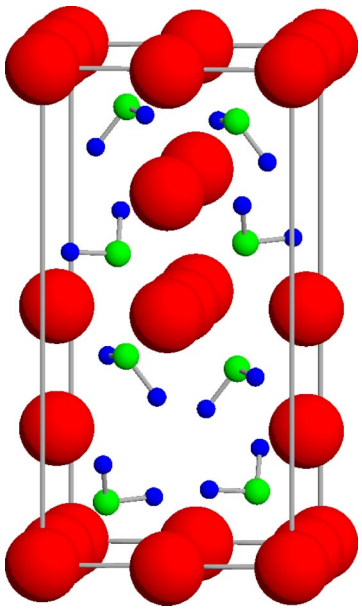

FIG. 1. (Color online) Crystal structure of $LiNH_2$. Red (large), green (middle), and blue (small) spheres represent Li, N, and H atoms, respectively.

TABLE I. Structural parameters of $LiNH_2$. Space group: $I\bar{4}$ (No. 82). The values in parentheses are the experimental data in Ref. 24.

Lattice parameters (Å)		Atom parameters							
			Position	x		y		z	
$a=5.079$	(5.037)	Li1	2*a*	0		0		0	
$c=10.113$	(10.278)	Li2	2*c*	0		1/2		1/4	
		Li3	4*f*	0		1/2		0.0018	(0.0042)
		N	8*g*	0.2253	(0.2284)	0.2480	(0.2452)	0.1155	(0.1148)
		H1	8*g*	0.2392	(0.226)	0.1337	(0.149)	0.1999	(0.172)
		H2	8*g*	0.3949	(0.308)	0.3603	(0.359)	0.1198	(0.114)

II. METHOD

The present calculations have been performed using the ultrasoft pseudopotential method[16] based on density functional theory.[17] The generalized gradient approximation proposed by Perdew, Burke, and Ernzerhof[18] is used for the exchange-correlation energy.

All pseudopotentials are constructed from the results of scalar-relativistic all-electron calculations.[19] The pseudowave functions and the pseudoaugmentation charge functions are optimized by a method similar to that proposed by Rappe *et al.*[20] For nitrogen, the 2*s* and 2*p* states are chosen as the reference states where double projector functions are employed for each component and the 3*d* state as the local part of pseudopotential. The pseudopotentials for H and Li are the same as those used in Ref. 12. The details of computational procedure for the self-consistent-field calculation and the structural relaxation are described in Refs. 21 and 22. The computational methods to obtain the dielectric and vibrational properties can be found in Refs. 12 and 23.

The cutoff energies used here are 15 and 120 hartrees for the pseudowave functions and the charge density, respectively. The *k*-point grids for the Brillouin zone integration are generated so as to make the edge lengths of the grid elements closer to the target value of 0.08 $bohr^{-1}$ as possible. We have checked that these conditions give good convergence of the total energy within 1 meV/atom.

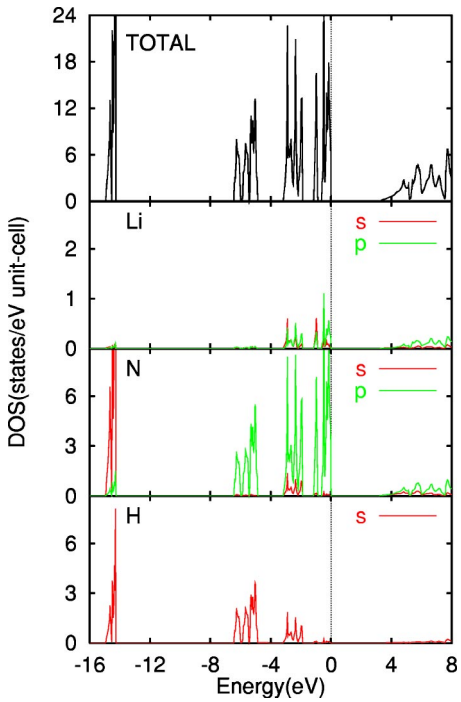

FIG. 2. (Color online) Total and partial densities of states for $LiNH_2$. The origin of the energy is set to be the top of the valence states.

III. RESULTS AND DISCUSSION

A. Lithium amide

The crystal structure of $LiNH_2$ is shown in Fig. 1. The symmetry is tetragonal with space group $I\bar{4}$. Two hydrogen atoms form an amide ion with a nitrogen atom, which has a bent shape. The calculated structural parameters are given in

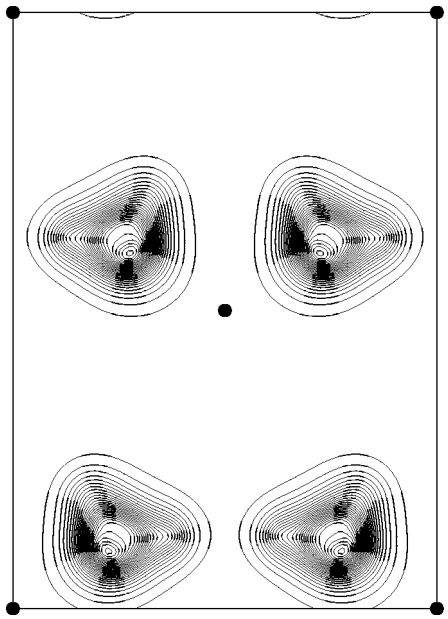

FIG. 3. Valence charge contour plot for $LiNH_2$ in the (110) plane. The contour space is 0.02 $e/bohr^3$. Solid circles denote Li atoms located on the plane. Note that the positions of N and H atoms are slightly shifted from the plane.

TABLE II. Dielectric properties of $LiNH_2$. Macroscopic high-frequency dielectric permittivity tensors ε_∞ and Born effective charge tensor Z^*.

	xx	*yy*	*zz*	*xy*	*yz*	*zx*	*xz*	*zy*	*yx*
ε_∞	2.75	2.75	2.83	0	0	0	0	0	0
Z^*_{Li1}	0.94	0.94	0.93	0.02	0	0	0	0	−0.02
Z^*_{Li2}	0.89	0.89	0.91	0.01	0	0	0	0	−0.01
Z^*_{Li3}	0.90	0.92	0.91	−0.03	0	0	0	0	−0.03
Z^*_{N}	−1.06	−1.32	−1.19	0.15	0.07	0.09	0.07	−0.20	0.15
Z^*_{H1}	0.23	0.16	0.04	−0.01	0.15	−0.07	−0.08	0.15	0.01
Z^*_{H2}	−0.11	0.27	0.23	−0.10	0.03	−0.11	−0.08	0.02	−0.13

Table I, together with the experimental data.[24] The agreement with the experimental data is very good except for hydrogen positions. The bond length between N and H is predicted as 1.03 Å, which coincides with a typical N-H bond length of 1.01 Å in an NH_3 molecule. The experimental bond length (0.70, 0.76 Å) is considerably shorter than these values. This discrepancy might be caused by the experimental difficulty in identifying hydrogen positions. The calculated H-N-H bond angle is 102.4°.

Figure 2 depicts total and partial densities of states for $LiNH_2$. The electronic structure is nonmetallic with a calculated energy gap of 3.2 eV. As expected, the contribution of Li orbitals to the occupied states is considerably small and therefore Li atoms are thought to be ionized as Li^+ cations. The occupied states mainly consist of N 2*s*, N 2*p*, and H 1*s* orbitals and form sharp peaks, suggesting that they are strongly localized around $[NH_2]^-$ anions. The lowest-energy state is composed of N 2*s* and H 1*s* states. In the middle-energy region, N 2*p* orbitals hybridize with H 1*s* orbitals. At the top of the occupied states, N 2*p* orbitals are dominated which have a nonbonding character. These bonding properties are similar to those of an H_2O molecule. As seen for $LiBH_4$, a deficient electron to form the internal bonding of an $[NH_2]^-$ anion is compensated by a Li^+ cation. The valence charge contour plot is shown in Fig. 3. The valence charge density around the Li atoms is considerably low. The charge density is strongly localized around the $[NH_2]^-$ anions and there are no overlaps between them.

The results of the dielectric properties for $LiNH_2$ are listed in Table II, which are used to calculate the dipole-dipole interactions induced by atomic displacements in the lattice dynamics. The macroscopic high-frequency dielectric permittivity tensor ε_∞ is diagonal due to the tetragonal symmetry of crystal, where $\varepsilon_{\infty,xx}=\varepsilon_{\infty,yy}$. The difference between $\varepsilon_{\infty,xx}$ ($\varepsilon_{\infty,yy}$) and $\varepsilon_{\infty,zz}$ is less than 3% and so the anisotropy of ε_∞ is small.

The Born effective charge tensors are useful to consider the bonding characters of materials. It is thought to be a good indicator to measure an ionic nature of elements because the definition is theoretically clear and, in principle, it has the exact value. For Li, the diagonal elements of the Born effective charge tensor are $Z^*_{\mathrm{Li}}=0.89-0.93$ which are close to the ideal value of +1 and absolute values of the off-diagonal elements are relatively small. This supports an ionic picture for the bonding between the Li and NH_2 units. Small absolute values for the diagonal elements of Z^*_{H} indicate little ionic character between N-H bonds. The internal bonding of $[NH_2]^-$ anions is thought to be primarily covalent.

The optical Γ-phonon frequencies are given in Table III. There are 45 optical Γ-phonon modes because the unit cell contains four formula units. The irreducible representation of them is $10A+11B+24E$; the *B* and *E* modes are both infrared and Raman active, and the *A* mode is Raman active. The infrared-active modes are divided into transverse optical (TO) modes and longitudinal optical (LO) modes due to the dipole-dipole interactions. Analyzing the eigenvectors, we confirm that the eigenmodes around 1500 and 3400 cm^{-1} originate from the internal N-H bending and stretching vibrations of $[NH_2]^-$ anions, respectively. The TO-LO splitting for the N-H stretching modes is essentially negligible because of little ionic character between N-H bonds. The results of our Raman spectroscopy measurements[25] are 3260 and 3320 cm^{-1}. Recent infrared spectroscopy experiments[26] show IR bands at 3260 and 3315 cm^{-1}. The predicted values for the N-H stretching modes agree well with these experimental results. For comparison purposes, we have calculated the vibrational frequencies of a free $[NH_2]^-$ anion using an fcc supercell with $a=12$ Å, where the extra negative charge

TABLE III. Optical Γ-phonon frequencies (in cm^{-1}) of $LiNH_2$.

Modes	Frequencies											
A	239	282	316	344	397	515	655	1514	3392	3470		
B (TO)	192	281	311	336	417	464	588	701	1507	3400	3468	
B (LO)	196	301	328	348	454	531	607	702	1512	3400	3468	
E (TO)	116	225	249	293	316	378	499	565	677	1462	3397	3466
E (LO)	118	238	254	301	325	484	536	585	677	1464	3397	3467

TABLE IV. Structural parameters of Li_3N. Space group: $P\bar{3}m1$ (No. 164).

Lattice parameters (Å)	Atom parameters				
		Position	x	y	z
$a=3.612$	Li1	1b	0	0	1/2
$c=3.847$	Li2	2d	1/3	2/3	0.0304
	N	1a	0	0	0

is compensated by the uniform background charge. The calculation gives a frequency of 1438 cm^{-1} for the bending mode and 3271 and 3366 cm^{-1} for the stretching modes. The molecular approximation is fairly good for the internal vibrations of $[NH_2]^-$ anions in $LiNH_2$, implying a strong internal bonding of them.

B. Lithium nitride

In order to obtain the heat of hydrogenation for the overall reaction in Eq. (1), we have also carried out the calculations on Li_3N. The crystal structure of Li_3N at ambient conditions has been reported[27] to be hexagonal with space group $P6/mmm$, where the lattice constants are $a=3.648$ Å and $c=3.875$ Å, and the atomic positions are the 1b and 2d sites for Li and the 1a site for N. Although the calculated lattice constants ($a=3.619$ Å and $c=3.847$ Å) agree well with the experimental values, we have found a weak soft mode of $65i$ cm^{-1} for this crystal structure. The soft mode has B_{2g} symmetry and the eigenvector corresponds to displacements of Li atoms at the 2d site along the c axis in opposite directions. When the soft mode is frozen, the symmetry is reduced to $P\bar{3}m1$. The structural parameters obtained for this symmetry are given in Table IV. Setting the atomic position of Li atoms at the 2d site to be $z=0$, the crystal symmetry returns to the reported one. The energy gain of the transition from $P6/mmm$ to $P\bar{3}m1$ is only 0.1 meV/atom. Since this energy gain and the atomic displacements are very small, the low-symmetry phase with $P\bar{3}m1$ is most likely suppressed by thermal atomic motions at room temperature. The optical Γ-phonon frequencies for the low-symmetry phase are summarized in Table V, where the dielectric properties given in Table VI are used to add the dipole-dipole interactions for the infrared active modes. The lowest A_{1g} mode corresponds to the soft mode found for $P6/mmm$ symmetry. The changes in frequencies of other modes due to the structural transition are less than 10 cm^{-1}.

TABLE V. Optical Γ-phonon frequencies (in cm^{-1}) of Li_3N with $P\bar{3}m1$ symmetry.

Modes	Frequencies	
A_{1g}	98	
A_{2u} (TO)	488	678
A_{2u} (LO)	501	731
E_g	611	
E_u (TO)	328	419
E_u (LO)	350	564

TABLE VI. Dielectric properties of Li_3N with $P\bar{3}m1$ symmetry. Macroscopic high-frequency dielectric permittivity tensors ε_∞ and Born effective charge tensor Z^*. The yy element is the same as xx and all off-diagonal elements are equal to zero due to the symmetry for all tensors.

	xx	zz
ε_∞	6.10	5.45
Z^*_{Li1}	0.87	1.00
Z^*_{Li2}	0.90	0.40
Z^*_N	−2.67	−1.79

Considering the results for the density of states and the valence charge distribution (not shown[28]), the bonding character of this material seems to be ionic. The electronic structure is nonmetallic with a calculated energy gap of 1.1 eV and the occupied states are mainly composed of N orbitals. The valence charge density is spherically localized around N atoms and is hardly seen around Li atoms. However, the Born effective charge tensors shown in Table VI give somewhat different natures. For Li at the 2d site and N, large anisotropies are found and their zz components deviate remarkably from the ideal values. The Born effective charge tensors for the $P6/mmm$ phase are essentially the same as those given in Table VI. The anisotropic polarizability for N in Li_3N has been also suggested from an analysis for lattice dynamics using a rigid-shell model.[29] The large deviations from the ideal values indicate that the bonding character of Li_3N is partially covalent, not purely ionic.

C. Heat of formation

The heat of formation is the most fundamental and important quantity for hydrogen storage materials, which can be estimated from the difference between the energies before and after the hydriding reaction. In Table VII, we summarize the cohesive energies as well as the zero-point energies for the materials related to the overall reaction in Eq. (1), where the zero-point energies are calculated within the harmonic approximation. A supercell containing 16 formula units is used for Li_3N to obtain the phonon density of states. For $LiNH_2$, the zero-point energy is estimated from only the

TABLE VII. Calculated cohesive energies E_{coh} (eV/atom) and zero-point energies E_{zero} (meV/atom). Note that the zero-point energies are not included in E_{coh}.

	E_{coh}	E_{zero}
$LiNH_2$	3.26	179
Li_3N	2.83	74
H_2[a]	2.27	135
LiH[a]	2.36	111

[a]Reference 12.

Γ-phonon eigenmodes, since the high-frequency internal bending and stretching modes of $[NH_2]^-$ anions can be fairly reproduced by the molecular approximation, which are expected to have the dominant contributions.

The heat of formation for the overall reaction in Eq. (1) is predicted as −99 kJ/mol H_2 when considering only the total energies and −85 kJ/mol H_2 including the zero-point energy contributions. The predicted value with the zero-point energy contributions agrees well with the experimental value[11] of −81 kJ/mol H_2. From the practical point of view, the value of about −80 kJ/mol H_2 means that the hydride phase is too stable for applications. To lower the dehydriding temperature, it is required to make the heat of formation less negative. Therefore, the partial substitution of more electronegative elements for Li, which has been proposed for $LiBH_4$ to lower the dehydriding temperature, is also expected to be effective for the destabilization of $LiNH_2$. The effect of the cation substitution has been examined for $LiNH_2$ experimentally.[14,31]

Understanding the properties of the intermediate phase of the hydriding reaction in Eq. (1), lithium imide, Li_2NH, is also of great interest. The crystal structure of Li_2NH was reported[30] to be antifluorite type consisting of Li^+ and $[NH]^{2-}$. However, hydrogen positions were not determined. In this connection, the structure of Li_2NH has been recently investigated by neutron powder diffraction[32] and synchrotron powder x-ray diffraction,[33] from which crystal structure models have been proposed. A theoretical investigation of the structural and other fundamental properties of Li_2NH is now in progress.[34]

IV. SUMMARY

First-principles calculations have been performed on lithium amide, $LiNH_2$, using the ultrasoft pseudopotential method to predict its fundamental properties: the structural, electronic, dielectric, and vibrational properties. The several analyses suggest that an $[NH_2]^-$ anion in $LiNH_2$ forms strong internal bonds with a covalent character. A deficient electron to form them is compensated for by a Li^+ cation. These bonding natures are quite similar to those of $LiBH_4$.[12]

ACKNOWLEDGMENTS

We would like to thank T. Noritake, M. Aoki, G. Kitahara, Y. Kojima, and S. Hyodo for valuable discussions. This study was partially supported by the New Energy and Industrial Technology Development Organization (NEDO), Basic Technology Development Project of Hydrogen Safety and Utilization (2003-2004).

*Electronic address: miwa@cmp.tytlabs.co.jp

[1] B. Bogdanović and M. Schwickardi, J. Alloys Compd. **253**, 1 (1997).
[2] R. A. Zidan, S. Takara, A. G. Hee, and C. M. Jensen, J. Alloys Compd. **285**, 119 (1999).
[3] L. Zaluski, A. Zaluuka, and J. O. Ström-Olsen, J. Alloys Compd. **290**, 71 (1999).
[4] K. J. Gross, S. Guthrie, S. Tanaka, and G. Thomas, J. Alloys Compd. **297**, 270 (1999).
[5] B. Bogdanović, R. A. Brand, A. Marjanović, M. Schwickardi, and J. Tölle, J. Alloys Compd. **302**, 36 (2000).
[6] C. M. Jensen and K. J. Gross, Appl. Phys. A: Mater. Sci. Process. **72**, 213 (2001).
[7] D. Sun, T. Kiyobayashi, H. Takeshita, N. Kuriyama, and C. M. Jensen, J. Alloys Compd. **337**, L8 (2002).
[8] G. P. Meisner, G. G. Tibbetts, F. E. Pinkerton, C. H. Olk, and M. P. Balogh, J. Alloys Compd. **337**, 254 (2002).
[9] G. Sandrock, K. Gross, and G. Thomas, J. Alloys Compd. **339**, 229 (2002).
[10] H. Morioka, K. Kakizaki, S.-C. Chung, and A. Yamada, J. Alloys Compd. **353**, 310 (2003).
[11] P. Chen, Z. Xiong, J. Luo, J. Lin, and L. Tan, Nature (London) **420**, 302 (2002).
[12] K. Miwa, N. Ohba, S. Towata, Y. Nakamori, and S. Orimo, Phys. Rev. B **69**, 245120 (2004).
[13] K. Miwa, N. Ohba, S. Towata, Y. Nakamori, and S. Orimo, J. Alloys Compd. (to be published).
[14] S. Orimo, Y. Nakamori, G. Kitahara, K. Miwa, N. Ohba, T. Noritake, and S. Towata, Appl. Phys. A: Mater. Sci. Process. **79**, 1765 (2004).
[15] B. A. Boukamp and R. A. Huggins, Mater. Res. Bull. **13**, 23 (1978).
[16] D. Vanderbilt, Phys. Rev. B **41**, R7892 (1990); K. Laasonen, A. Pasquarello, R. Car, C. Lee, and D. Vanderbilt, *ibid.* **47**, 10142 (1993).
[17] P. Hohenberg and W. Kohn, Phys. Rev. **136**, B864 (1964); W. Kohn and L. J. Sham, Phys. Rev. **140**, A1133 (1965).
[18] J. P. Perdew, K. Burke, and M. Ernzerhof, Phys. Rev. Lett. **77**, 3865 (1996); **78**, 1396(E) (1997).
[19] D. D. Koelling and B. N. Harmon, J. Phys. C **10**, 3107 (1977).
[20] A. M. Rappe, K. M. Rabe, E. Kaxiras, and J. D. Joannopoulos, Phys. Rev. B **41**, R1227 (1990).
[21] A. Fukumoto and K. Miwa, Phys. Rev. B **55**, 11155 (1997).
[22] K. Miwa and A. Fukumoto, Phys. Rev. B **65**, 155114 (2002).
[23] N. Ohba, K. Miwa, N. Nagasako, and A. Fukumoto, Phys. Rev. B **63**, 115207 (2001).
[24] Von H. Jacobs and R. Juza, Z. Anorg. Allg. Chem. **391**, 271 (1972).
[25] Y. Nakamori and S. Orimo, J. Alloys Compd. **370**, 271 (2004).
[26] Y. Kojima and Y. Kawai, Chem. Commun. (Cambridge) **2004**, 2210 (2004).
[27] A. Rabenau and H. Schulz, J. Less-Common Met. **50**, 155 (1976).
[28] The detailed charge density analysis as well as the density of states for Li_3N can be found in the following reference: G. Kerker, Phys. Rev. B **23**, 6312 (1981).
[29] H. R. Chandrasekhar, G. Bhattacharya, R. Migoni, and H. Bilz, Phys. Rev. B **17**, 884 (1978).

[30] R. Juza and K. Opp, Z. Anorg. Allg. Chem. **266**, 325 (1951).
[31] Y. Nakamori and S. Orimo, J. Alloys Compd. **370**, 271 (2004).
[32] K. Ohoyama, Y. Nakamori, S. Orimo, and K. Yamada, J. Phys. Soc. Jpn. **74**, 483 (2005).
[33] T. Noritake, H. Nozaki, M. Aoki, S. Towata, G. Kitahara, Y. Nakamori, and S. Orimo, J. Alloys Compd. **393**, 264 (2005).
[34] We deduce from our survey calculations that the heat of formation for the second-step reaction in Eq. (1), $Li_2NH + H_2 \leftrightarrow LiNH_2 + LiH$, is about −70 kJ/mol H_2, which is in fairly good agreement with the recent experimental value of −60 kJ/mol H_2 [W. Luo, J. Alloys Compd. **385**, 316 (2004)].